For morphometry of axonal degeneration in the sciatic nerves and SYP-immunoreactive aberrant dot-like structures in the cerebellar molecular layer, photomicrographs were taken with a digital camera attached to a microscope (DP71, Olympus Corp., Tokyo, Japan). Measurement was then performed using image analysis software (WinROOF, Version 5.7.1, Mitani Corp. Tokyo, Japan). The total number of axons/unit area and the numbers of degenerated axons and the diameters of axons were assessed in one cross-sectional area at 400× magnification of toluidine blue-stained specimens from each animal, and the density, percentage of degenerated axons, and percentage of myelinated axons less than 3 μm in diameter were calculated. For evaluation of SYP-immunoreactive aberrant dot-like structures, numbers of dots in the left cerebellar hemisphere were counted following measurement of the length of the cortex in one cross-sectional area at 12.5× magnification and the number of SYP-immunoreactive dots/unit length of the cortex was calculated.

For testicular toxicity, approximately 400–650 circularly sectioned seminiferous tubules for each rat were assessed microscopically, and then the percentages of tubules with histopathological changes were calculated.

Comet assay

The procedures for preparing and processing comet assays were performed according to the recommendation by an expert working group on the comet assay in the International Workshop on Genotoxicity Testing (IWGT) (Tice et al. 2000; Burlinson et al. 2007) and slightly modified for testes. Briefly, each testis was washed with cold mincing/homogenizing buffer containing Hanks' Balanced Salt (HBSS) Solutions (Invitrogen Corporation, Carlsbad, CA, USA), 20 mM EDTA·2Na, and 10% DMSO, minced with scissors, and placed on ice for 15–30 s to precipitate clumps of cells. The supernatant was suspended in 0.5% Nusieve GTG agarose (Lonza, Basel, Switzerland), quickly layered on a MAS-coated slide (Matsunami Glass Ind. Ltd., Osaka, Japan), immersed in lysing solution (pH10, 100 mM EDTA·2Na, 2.5 M NaCl, 10 mM Tris(hydroxymethyl)aminomethane containing 1% Triton-X and 10% DMSO) at 4°C overnight, and electrophoresed for 15 min in alkaline buffer after the unwinding treatment. Then, the cells were fixed with ethanol and stained with SYBER green (Molecular Probes, Eugene, OR, USA) according to the manufacturer's recommendation. We observed the cells under a fluorescence microscope (BX50, Olympus Co.). Round-shaped cells, considered as spermatocytes and early spermatids, were captured with a CCD camera. At least 100 cells were observed and the tail intensity of each comet image was measured using an image analysis software (Comet assay IV, Perceptive Instruments Ltd., Suffolk, UK).

Micronucleus (MN) test

The MN test for the testis was conducted according to the method of Tates et al. (1983) with a slight modification. Briefly, the testes excised from each animal were minced in HBSS Solution. The cell suspensions were incubated in 2 mg/ml collagenase solution (Wako Pure Chemicals Ind., Osaka, Japan) for 30 min at 37°C in a shaking water bath, filtered through a cell strainer, washed, and fixed in methanol. The cells were stained with DAPI (4′,6-diamidino-2-phenylindole dihydrochloride), and the slide specimens were prepared with acridine orange coating (TOYOBO Co., Ltd., Tokyo, Japan). We observed 1,000 early spermatids per animal under a fluorescence microscope (BX50, Olympus Co.).

Measurement of GST activity and GSH content

The livers and testes obtained from the satellite groups were rinsed with PBS solution to remove any red blood cells. Total GSH concentrations were determined with the Glutathione Assay Kit (Cayman Chemical, Ann Arbor, MI, USA), and GST activity was measured using a Glutathione *S*-Transferase Assay Kit (Cayman Chemical). Sample preparation and measurement were conducted according to the instructions of the manufacturer.

Statistical analysis

Variance in data for body weights, food consumption, water consumption, values from morphometric assessment in the sciatic nerves, cerebellar molecular layer and testis, and data for the comet assay were checked for homogeneity by Bartlett's procedure. If the variance was homogeneous, the data were assessed by one-way analysis of variance. If not, the Kruskal–Wallis test was applied. When statistically significant differences were indicated, the Dunnett's multiple test was employed for comparisons between the 0 ppm and ACR-treated groups. Data for the MN tests, GST activity, and GSH content were analyzed by Student's or Welch's t test following a test for equal variance.

Results

In-life parameters and intake of ACR

Suppression of body weight gain was observed in the young groups at 100 and 200 ppm from week 2 (Fig. 1a).

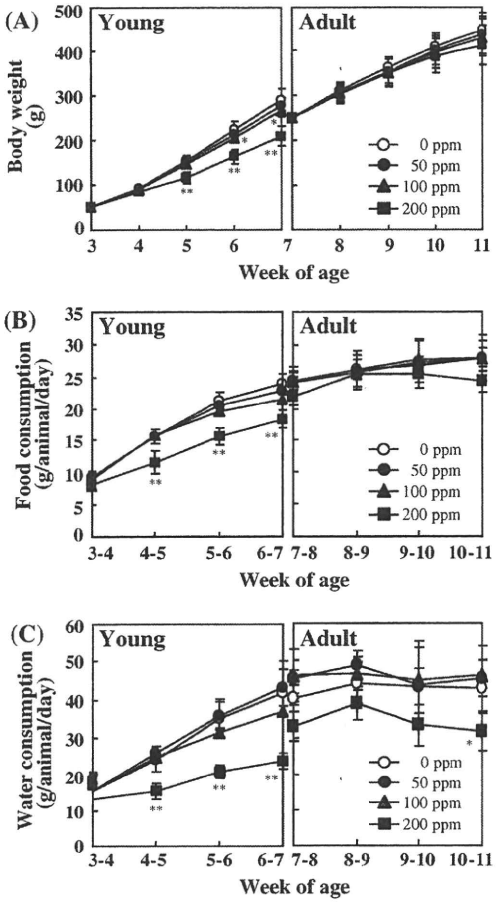

Fig. 1 Time course of change in body weights (**a**), food consumption (**b**), and water consumption (**c**) in young and adult rats given ACR in the drinking water for 4 weeks. Data are mean ± SD. *, **$P < 0.05$ and $P < 0.01$ vs. 0 ppm

In the adult groups, there were no intergroup differences in the body weight curves. Also, food consumption was suppressed only in the young group at 200 ppm (Fig. 1b). Water consumption was lowered at 200 ppm both in young and adult groups (Fig. 1c). Mean daily intakes of ACR are summarized in Table 1. Compared to adult groups, mean daily intake of ACR per kg body weight was higher in young groups at each dose.

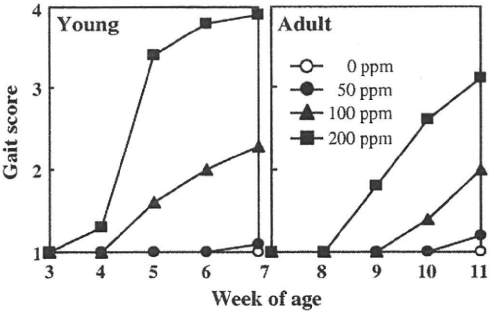

Fig. 2 Scores for gait abnormalities of young and adult rats given ACR in the drinking water for 4 weeks

Both in young and adult groups, apparent gait abnormalities were found at 100 and 200 ppm, and their severity advanced during the exposure in a dose-dependent manner (Fig. 2). Young groups showed earlier occurrence of gait abnormalities and faster progression of the symptoms than adult groups. At 200 ppm, slightly abnormal gait appeared in the young animals from week 1, and symptoms rapidly progressed so that the gait score reached 3.4 at week 2. Adult animals at 200 ppm exhibited mild gait abnormality from week 2, which progressed to score 3.1 at week 4.

Final body and organ weights are summarized in Table 2. In young groups, body weights were significantly depressed at 100 and 200 ppm. Alteration of the brain weight in young rats appeared to reflect body weight decrease. Decreases in absolute weights of the testis and epididymides observed in young and adult rats could have been linked with the histopathological changes described below.

Morphometric analysis

Data for histopathology and morphometry of lesions developing in the nervous system are shown in Table 3. Representative histopathological illustrations of the nervous systems of young and adult groups are summarized in Fig. 3 and Fig. 4, respectively. In both young and adult groups, central chromatolysis of ganglion cells in the trigeminal nerves was apparent from 100 ppm. The density of

Table 1 Mean daily intake of ACR in young and adult rats

Group	Acrylamide in the drinking water (ppm)				
		0	50	100	200
	No. of animals examined	10	10	10	10
Young	(mg/kg/day)	0 ± 0[a]	8.27 ± 0.32	15.73 ± 1.51	26.37 ± 3.51
Adult	(mg/kg/day)	0 ± 0	6.26 ± 1.10	12.63 ± 1.97	19.07 ± 3.46

[a] Mean ± SD

Table 2 Body and organ weights of young and adult rats given ACR in the drinking water for 4 weeks

		Acrylamide in the drinking water (ppm)			
		0	50	100	200
Young					
Body weight	(g)	287.4 ± 24.6[a]	273.5 ± 15.7	263.7 ± 14.4*	210.4 ± 24.3**
Brain	(g)	1.97 ± 0.05	1.94 ± 0.09	1.83 ± 0.09*	1.66 ± 0.04**
	(g%)	0.69 ± 0.06	0.71 ± 0.05	0.69 ± 0.03	0.80 ± 0.08**
Testes	(g)	2.57 ± 0.15	2.44 ± 0.22	2.39 ± 0.19	1.87 ± 0.36**
	(g%)	0.90 ± 0.07	0.90 ± 0.09	0.91 ± 0.07	0.89 ± 0.12
Epididymides	(g)	0.40 ± 0.04	0.35 ± 0.02**	0.37 ± 0.04	0.30 ± 0.02**
	(g%)	0.14 ± 0.02	0.13 ± 0.01	0.14 ± 0.02	0.15 ± 0.02
Adult					
Body weight	(g)	444.3 ± 38.0	433.0 ± 42.0	426.7 ± 42.1	409.2 ± 45.5
Brain	(g)	2.07 ± 0.06	2.08 ± 0.11	2.02 ± 0.09	1.99 ± 0.07
	(g%)	0.47 ± 0.03	0.48 ± 0.04	0.48 ± 0.04	0.49 ± 0.06
Testes	(g)	3.30 ± 0.26	3.39 ± 0.39	3.25 ± 0.20	3.19 ± 0.24
	(g%)	0.74 ± 0.07	0.78 ± 0.08	0.77 ± 0.08	0.79 ± 0.09
Epididymides	(g)	0.97 ± 0.05	1.04 ± 0.09	0.97 ± 0.07	0.84 ± 0.06**
	(g%)	0.22 ± 0.02	0.24 ± 0.02	0.23 ± 0.03	0.21 ± 0.02

10 animals per each group were examined

[a] Mean ± SD

*, ** $P < 0.05$, $P < 0.01$ vs. 0 ppm group

Table 3 Histopathology and morphometry of lesions developing in the nervous system

		Acrylamide in the drinking water (ppm)			
		0	50	100	200
Young					
Trigeminal nerve					
No. of animals examined		10	10	10	10
Central chromatolysis (+/++/+++)[a]		0	3 (3/0/0)	10 (0/5/5)[##]	10(0/0/10)[##]
Sciatic nerve (distal portion)					
No. of animals examined		10	10	10	10
Density	(/100 μm^2)	2.56 ± 0.32[b]	2.73 ± 0.17	2.92 ± 0.25**	2.42 ± 0.25
Degenerated axons	(%)	0.28 ± 0.15	0.39 ± 0.14	0.82 ± 0.19**	7.51 ± 3.25**
Myelinated axons, <3 μm in diameter	(%)	18.01 ± 3.45	16.74 ± 2.79	18.80 ± 2.73	21.57 ± 4.07
Cerebellar cortex					
No. of animals examined		5	5	5	5
SYP-immunoreactive aberrant dots	(/mm cortex)	0.50 ± 0.20	0.41 ± 0.18	1.49 ± 0.59	6.09 ± 1.62*
Adult					
Trigeminal nerve					
No. of animals examined		10	10	10	10
Central chromatolysis (+/++/+++)[a]		0	3 (3/0/0)	10 (3/7/0)[##]	10 (0/3/7)[##]
Sciatic nerve (distal portion)					
No. of animals examined		10	10	10	10
Density	(/100 μm^2)	2.10 ± 0.23	2.03 ± 0.15	2.10 ± 0.24	2.15 ± 0.24
Degenerated axons	(%)	0.39 ± 0.16	0.65 ± 0.27	0.96 ± 0.37*	1.74 ± 0.77**
Myelinated axons, <3 μm in diameter	(%)	13.96 ± 2.75	12.30 ± 2.39	13.45 ± 2.68	14.16 ± 2.82
Cerebellar cortex					
No. of animals examined		5	5	5	5
SYP-immunoreactive aberrant dots	(/mm cortex)	0.54 ± 0.12	0.47 ± 0.09	1.71 ± 0.81	5.88 ± 2.61*

[a] *Grade of change* + mild, ++ moderate, +++ severe

[b] Mean ± SD

*, ** $P < 0.05$, $P < 0.01$ vs. 0 ppm group

[##] $P < 0.01$ vs. 0 ppm group (Fisher's exact test)

SYP synaptophysin

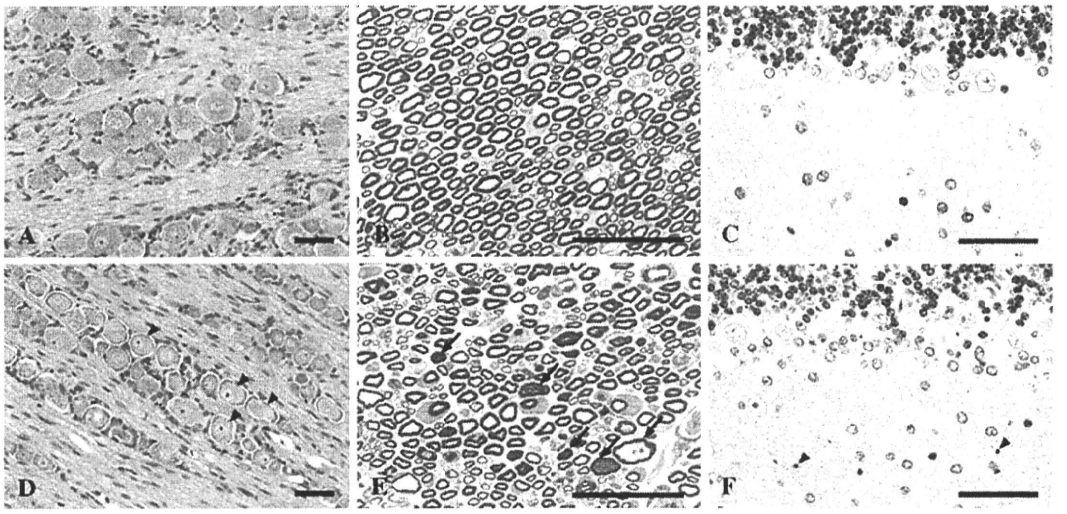

Fig. 3 Histopathology of the trigeminal nerve (**a**, **d**), sciatic nerve (**b**, **e**), and cerebellar molecular layer (**c**, **f**) in young rats given ACR at 0 or 200 ppm for 4 weeks. (**a–c**) Normal tissues of a young rat from the 0 ppm group. (**d–f**) At 200 ppm, central chromatolysis of ganglion cells (**d** *arrowheads*) in the trigeminal nerve was apparent. Increases in degenerated axons (**e** *arrows*) in the sciatic nerve and dot-like SYP-immunoreactive structures (**f** *arrowheads*) in the cerebellar molecular layer were also found. **a**, **d** hematoxylin and eosin. **b**, **e** resin-embedded semithin sections stained with toluidine blue. **c**, **f** immunohistochemical staining for SYP. *Bar* = 50 μm

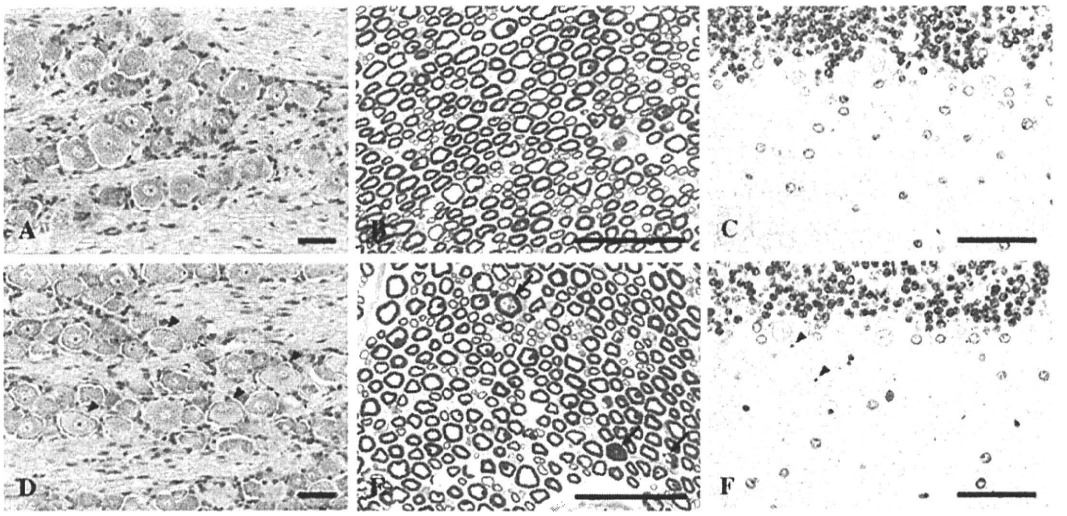

Fig. 4 Histopathology of the trigeminal nerve (**a**, **d**), sciatic nerve (**b**, **e**), and cerebellar molecular layer (**c**, **f**) of adult rats given ACR at 0 or 200 ppm for 4 weeks. (**a–c**) Normal tissues of an adult rat from 0 ppm group. (**d–f**) Similar to the young group, central chromatolysis of ganglion cells (**d** *arrowheads*) in the trigeminal nerve, increases in degenerated axons (**e** *arrows*) in the sciatic nerve and dot-like SYP-immunoreactive structures (**f** *arrowheads*) in the cerebellar molecular layer were observed at 200 ppm **a**, **d** hematoxylin and eosin. **b**, **e** resin-embedded semithin sections stained with toluidine blue. **c**, **f** immunohistochemical staining for SYP. *Bar* = 50 μm

axons in the sciatic nerve was increased only at 100 ppm in the young group, but without dose dependence. In both young and adult groups, significant increase in degenerated axons in the sciatic nerve was observed from 100 ppm, and increase in dot-like SYP-immunoreactive structures in the cerebellar molecular layer was also found at 200 ppm. Although not statistically significant, myelinated nerves <3 μm in diameter showed a tendency for increase at 200 ppm in both young and adult groups. At 200 ppm, most parameters were higher in young groups compared to adult counterparts.

In the testis, marked degeneration and loss of or decrease in spermatids was observed from 100 ppm in young animals (Fig. 5 and Table 4). Elongate spermatids

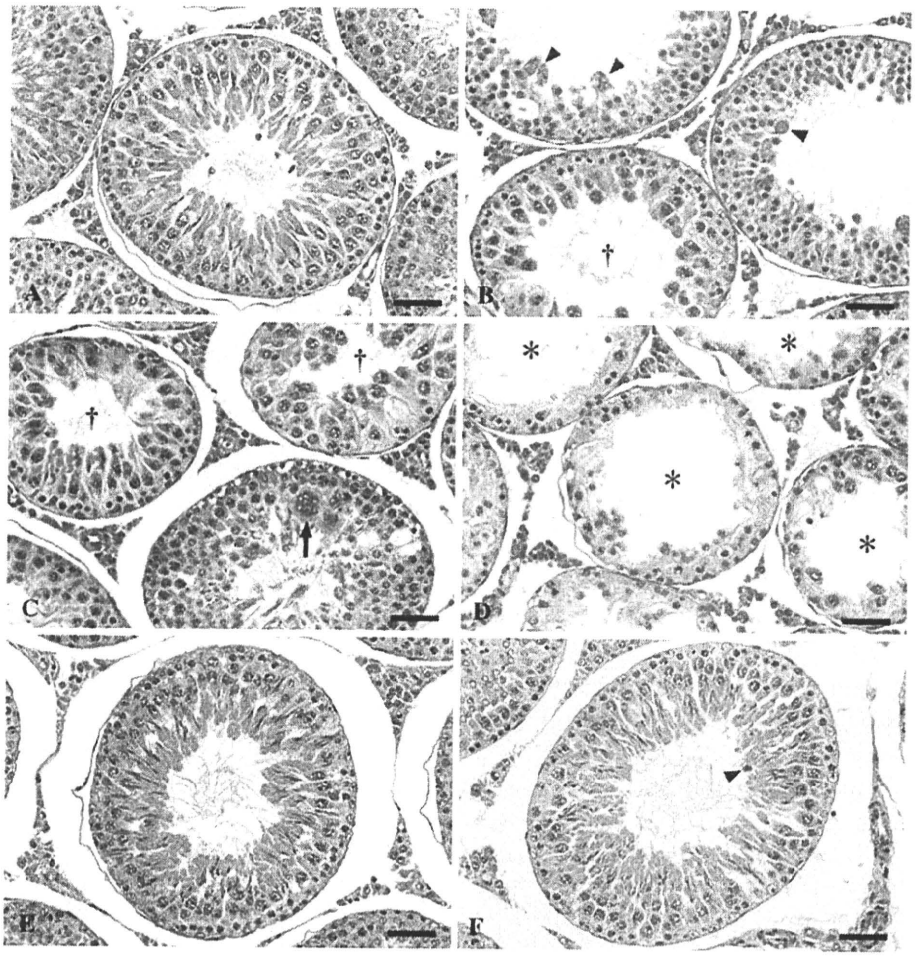

Fig. 5 Histopathology of the testis of young and adult rats given ACR at 0 or 200 ppm for 4 weeks. **a** Normal seminiferous tubules of a young rat from the 0 ppm group. (**b–d**) Degeneration of spermatids (*arrowheads*), loss of or decreased in elongated spermatids (†), and multinucleated giant cells (*arrow*) are apparent in a young rat at 200 ppm. In severely affected cases, many seminiferous tubules showed marked germ cell depletion (*). **e** Normal seminiferous tubules of an adult rat from the 0 ppm group. **f** Only a small number of exfoliated germ cells (*arrowhead*) was found in the lumina of tubules in a case of the adult group at 200 ppm. HE stain. All *bars* = 50 μm

appeared to be most vulnerable to ACR, and in severely affected cases, many seminiferous tubules showed marked germ cell depletion. In addition, exfoliation of germ cells and appearance of multinucleated giant cells were also found. Many exfoliated germ cells were observed in the epididymal duct. In the adult groups, only small numbers of exfoliated germ cells was found in lumina of seminiferous tubules. Sertoli cells were morphologically unaffected in both young and adult animals. Similar histopathological changes were also observed in the testis of each young and adult animal at 200 ppm in the satellite groups used for measuring GST activity and GSH contents.

Data for relationships between ACR intake per kg body weight and neurotoxicity parameters, including the gait score at week 4, the number of degenerated axons in the sciatic nerves, and the number of SYP-immunoreactive structures in the cerebellar molecular layer are shown in Fig. 6a–c. All these parameters increased in proportion to ACR intake. For testicular toxicity, the relationship between ACR intake per kg body weight and the percentage of affected seminiferous tubules is shown in Fig. 6d. With increase in ACR dose, affected tubules profoundly increased in the young group, while the magnitude of increase was very small in the adult group.

Comet assays and MN tests

The comet assay revealed that ACR significantly induced DNA damage in a dose-dependent manner from 100 ppm

Table 4 Histopathological data for the testes of young and adult rats given ACR in the drinking water for 4 weeks

Findings (%)[a]	Acrylamide in the drinking water (ppm)			
	0	50	100	200
Young				
Affected tubules[b]	3.51 ± 1.68[c]	9.03 ± 18.81	16.93 ± 12.23*	66.59 ± 26.96**
Exfoliation of germ cells	3.39 ± 1.61	3.93 ± 3.07	9.80 ± 6.22*	10.44 ± 9.87
Multinucleated giant cells	0.02 ± 0.06	0.07 ± 0.14	0.57 ± 0.71	1.67 ± 3.06**
Degeneration of spermatids	0.10 ± 0.18	0.84 ± 2.54	3.95 ± 6.47	20.90 ± 13.37**
Loss of or decrease in elongated spermatids	0 ± 0	4.99 ± 15.74*	5.62 ± 8.87**	20.43 ± 14.61**
Loss of or decrease in round spermatids	0.02 ± 0.06	0 ± 0	1.51 ± 3.19	12.68 ± 10.97**
Atrophic tubules[d]	0 ± 0	0.17 ± 0.54**	0.12 ± 0.38**	24.03 ± 30.83**
Sertoli cell vacuolation	0.60 ± 0.57	1.07 ± 0.55	0.99 ± 0.62	1.06 ± 0.92
Adult				
Affected tubules[b]	0.47 ± 0.30	0.58 ± 0.23	1.17 ± 0.60*	1.53 ± 0.67**
Exfoliation of germ cells	0.45 ± 0.30	0.56 ± 0.23	1.17 ± 0.60*	1.46 ± 0.71**
Multinucleated giant cells	0 ± 0	0 ± 0	0 ± 0	0.07 ± 0.17
Degeneration of spermatids	0 ± 0	0 ± 0	0 ± 0	0 ± 0
Loss of or decrease in elongated spermatids	0.02 ± 0.06	0.02 ± 0.07	0 ± 0	0 ± 0
Loss of or decrease in round spermatids	0 ± 0	0 ± 0	0 ± 0	0 ± 0
Atrophic tubules[d]	0 ± 0	0 ± 0	0 ± 0	0 ± 0
Sertoli cell vacuolation	0.62 ± 0.45	0.53 ± 0.50	0.72 ± 0.43	0.81 ± 0.53

10 animals per each group were examined

[a] Approximately 400–650 tubules/rat were examined

[b] Affected tubules represent total tubules with findings, except for tubules showing only Sertoli cell vacuolation

[c] Mean ± SD

[d] Atrophic tubules are those showing marked germ cell depletion

*, ** $P < 0.05$, $P < 0.01$ vs. 0 ppm group

in young and adult groups (Fig. 7a). Although the values did not greatly differ between the groups, the values in the young group were higher than those in the adult group at 200 ppm. On the other hand, MN was clearly induced only in young group in a dose-dependent manner (Fig. 7b) with statistical significance at both 100 and 200 ppm ($P < 0.05$). ACR slightly induced MN in the adult group at 200 ppm.

GST activity and GSH contents in the liver and testis

In the liver, compared to the 0 ppm group, GST activity was significantly increased at 200 ppm in the young group (Fig. 8a). Although not statistically significant, GST activity in the adult animals at 200 ppm also showed a tendency for increase. GSH contents were unchanged in both groups. There were no differences in the level of GST activity and GSH contents in the liver between young and adult groups. In the testis, although GST activity and GSH contents in both groups were not changed by ACR treatment, the levels of GST activity in the young group were significantly lower than those in the adult group (Fig. 8b).

Discussion

In the present study, ACR dose-related suppression of body weight, and food and water consumption was observed only in young rats. When gait abnormalities progressed, animals became unable to support their body weights, and it was difficult to take food and water from containers set in the upper part of the cage. Therefore, in the housing conditions designed for adult animals, the suppressions might be due to immature body size of young animals causing difficulty in access to food and water associated with the development of neurotoxicity.

On clinical observation, although both young and adult animals exhibited similar symptoms from 100 ppm, earlier occurrence and faster progression of the symptoms were

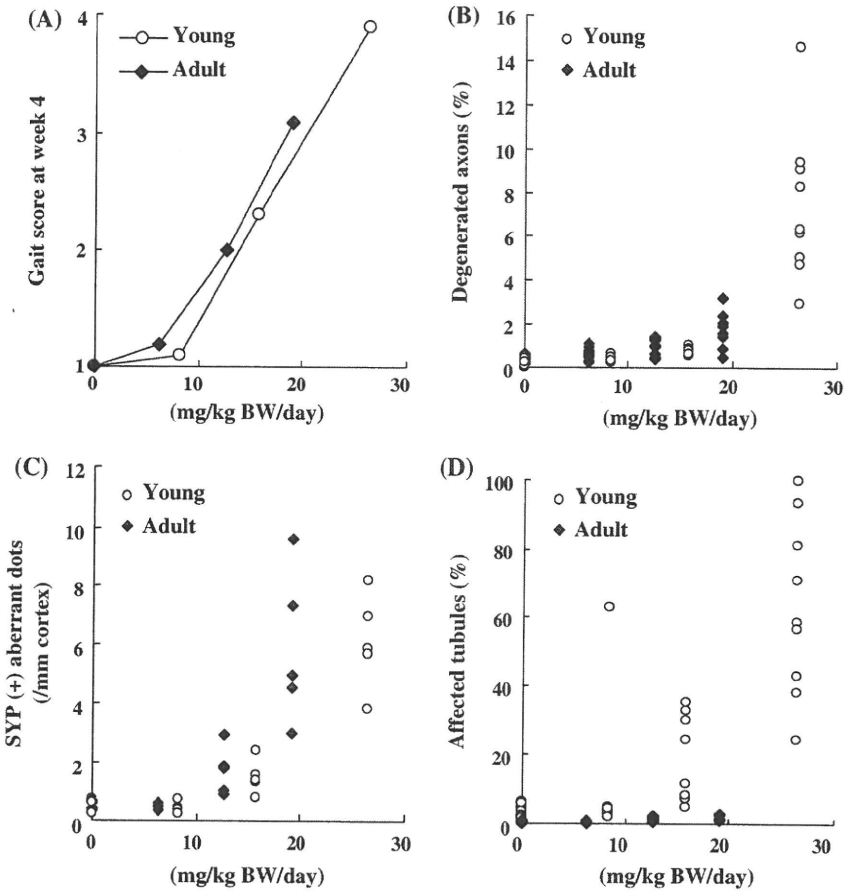

Fig. 6 Relationship between ACR intake per body weight and changes in neurotoxicity and testicular toxicity parameters in young and adult rats

here observed in the young group. Also, neurotoxic lesions such as central chromatolysis of ganglion cells in the trigeminal nerves, degenerated axons in the sciatic nerve and dot-like SYP-immunoreactive structures in the cerebellar molecular layer, were evident from 100 ppm in both young and adult groups. The magnitude of changes in these parameters was higher in the young group than in the adult group, especially at the highest dose, and neurotoxicity appeared stronger in young animals, though the types of lesions observed were similar between the young and adult groups. Compared to adult animals, intake of ACR per kg body weight was higher in young animals at each dose and the parameters indicating the neurotoxicity increased in proportion to ACR intake. Accordingly, the stronger neurotoxicity in the young animals can be considered to be a reflection of larger amount of ACR intake per body weight. These results suggest that the susceptibility to ACR-induced neurotoxicity in young and adult rats is qualitatively similar under the given experimental conditions. As mentioned in the Introduction section, a few studies have demonstrated life stage-related differences in susceptibility to ACR neurotoxicity, though the experimental conditions, such as age of animals, dosing methods, and parameters examined, were different. While Suzuki and Pfaff concluded that suckling rats were more susceptible (Suzuki and Pfaff 1973), it seems that there was not much difference in number of injections to cause apparent symptoms and myelin degeneration between suckling and adult rats. In the report by Ko et al., earlier occurrence and faster progression of neurological abnormalities in young animals were similar to those observed in our study (Ko et al. 1999). Although the authors stated that the daily intake was not significantly different between the young and adult groups, intake of ACR per body weight at the beginning of the experiment might have been higher in the young group, because younger animals usually take more water than older ones. Taken together, clear evidence of the susceptibility difference in neurotoxicity between young and adults animals is considered to be undetermined.

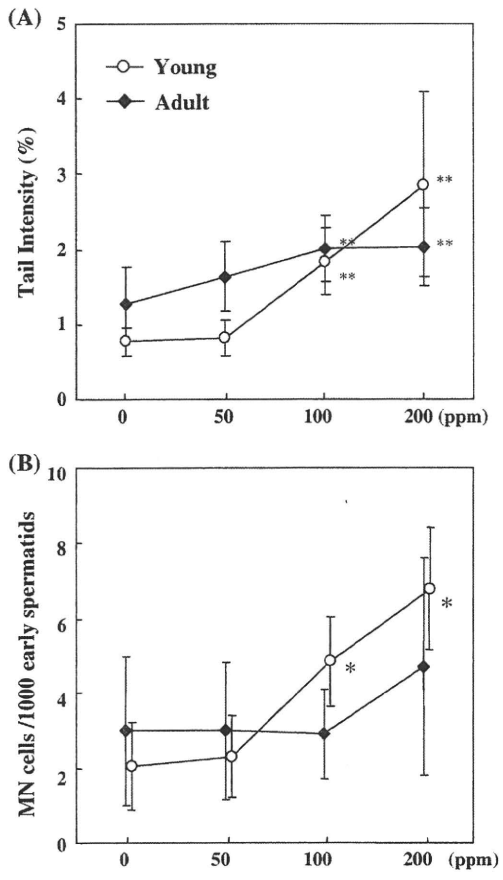

Fig. 7 Tail intensity of the comet image (**a**) and micronuclei frequency (**b**) obtained from young and adult rats given ACR in the drinking water for 4 weeks. Data are mean ± SD. $^{**}P < 0.01$ vs. 0 ppm

Regarding the susceptibility to ACR testicular toxicity in the present study, young animals showed apparently diverse and more profound lesions exceeding the dose–effect relationship observed in adult animals. ACR is known to interfere with motor proteins such as kinesin found in the sperm flagellum and alkylate protein sulfhydryl groups in the sperm tail (Sickles et al. 2007; Friedman et al. 2008). Therefore, it is considered that elongate spermatids are highly susceptible to ACR. In the comet assay, although DNA damage in the young group was higher than that in the adult group at 200 ppm, the values were not greatly different. However, the MN test revealed that ACR clearly induced MN in the young group, but not in the adult group. These results well correspond with the observations on histopathological examination. Because the comet assay and MN test in the testis target spermatocytes and early spermatids, the late stage of spermatogenesis may be more susceptible to ACR-induced genotoxicity in young than in adult animals.

As reported by others (Yousef and El-Demerdash 2006), the basal level of testicular GST activity in our cases was much lower than that in the liver. Although there were no life stage differences in the liver levels of GST activity, testicular GST activity in the present study was significantly lower in the young groups, irrespective of the ACR treatment. The activity of GST is low at birth and then increases gradually, but it has been known that the developmental profiles of antioxidant enzymes including GST in the testis differ greatly from those in the liver (Peltola et al. 1992). A study of the immunolocalization of GST-Yo, a member of the mu class expressed at high levels in the testis and epididymides, revealed that this enzyme was not detectable until 39 days of age and then appeared mainly in the elongate spermatids, with expression reaching maturity by day 49 (Papp et al. 1994). Therefore, the detoxification capacity of the testis in young animals was considered to be much lower than that in the adult animals during the experimental period in the present study, and such a difference might reasonably account for the high susceptibility to ACR-induced testicular toxicity observed in our young animals. In the liver, although GST activity was increased at 200 ppm, there were no apparent life-stage differences. Considering that the liver is the main organ involved in detoxification of ACR, similar level of GST activity may have contributed to the lack of differences in susceptibility to neurotoxicity between young and adult rats. Increase in GST activity in ACR-treated rats has been reported and considered to be due to increased formation of S-conjugates between ACR and GSH (Yousef and El-Demerdash 2006). ACR is known to cause GSH depletion (Zhang et al. 2009); however, decrease in GSH contents was not found in the present study. Because recovery or rather increase in liver GSH contents after depletion by treatment animals with acetaminophen has been reported (Ishii et al. 2009), the level of GSH in the present study might possibly have recovered after repeated treatment with ACR during the experimental period.

In summary, our results suggest that susceptibility to ACR neurotoxicity in young animals might not be different from that in adult ones when exposure levels are adjusted for the body weight. Regarding testicular toxicity, young animals proved more vulnerable than adults, and this might be due to a low level of testicular GST activity.

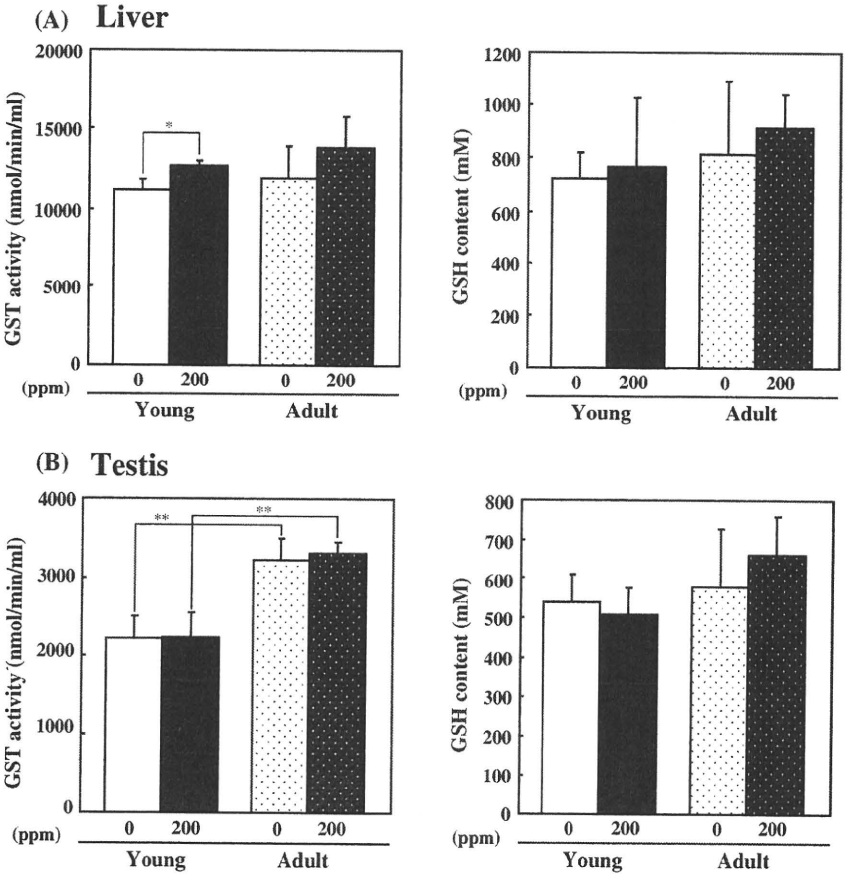

Fig. 8 GST activity and GSH contents in the liver (**a**) and testis (**b**) of young and adult rats given ACR at 0 or 200 ppm for 4 weeks. Data are mean ± SD. *, **$P < 0.05$ and $P < 0.01$

Acknowledgments This work was supported by Health and Labour Sciences Research Grants (Research on Food Safety) from the Ministry of Health, Labour and Welfare of Japan. We thank Miss Ayako Kaneko for technical assistance in conducting the animal study.

References

Burlinson B, Tice RR, Speit G, Agurell E, Brendler-Schwaab SY, Collins AR, Escobar P, Honma M, Kumaravel TS, Nakajima M, Sasaki YF, Thybaud V, Uno Y, Vasquez M, Hartmann A (2007) Fourth international workgroup on genotoxicity testing: results of the in vivo comet assay workgroup. Mutat Res 627:31–35

Exon JH (2006) A review of the toxicology of acrylamide. J Toxicol Environ Health B Crit Rev 9:397–412

Friedman MA, Zeiger E, Marroni DE, Sickles DW (2008) Inhibition of rat testicular nuclear kinesins (krp2; KIFC5A) by acrylamide as a basis for establishing a genotoxicity threshold. J Agric Food Chem 56:6024–6030

Ishii Y, Okamura T, Inoue T, Tasaki M, Umemura T, Nishikawa A (2009) Dietary catechol causes increased oxidative DNA damage in the livers of mice treated with acetaminophen. Toxicology 263:93–99

Kaplan ML, Murphy SD (1972) Effect of acrylamide on rotarod performance and sciatic nerve—glucuronidase activity of rats. Toxicol Appl Pharmacol 22:259–268

Ko MH, Chen WP, Lin-Shiau SY, Hsieh ST (1999) Age-dependent acrylamide neurotoxicity in mice: morphology, physiology, and function. Exp Neurol 158:37–46

Lee KY, Shibutani M, Kuroiwa K, Takagi H, Inoue K, Nishikawa H, Miki T, Hirose M (2005) Chemoprevention of acrylamide toxicity by antioxidative agents in rats–effective suppression of testicular toxicity by phenylethyl isothiocyanate. Arch Toxicol 79:531–541

Moser VC (1991) Investigations of amitraz neurotoxicity in rats. IV. Assessment of toxicity syndrome using a functional observational battery. Fundam Appl Toxicol 17:7–16

Papp S, Robaire B, Hermo L (1994) Developmental expression of the glutathione S-transferase Yo subunit in the rat testis and epididymis using light microscope immunocytochemistry. Anat Rec 240:345–357

Parzefall W (2008) Minireview on the toxicity of dietary acrylamide. Food Chem Toxicol 46:1360–1364

Peltola V, Huhtaniemi I, Ahotupa M (1992) Antioxidant enzyme activity in the maturing rat testis. J Androl 13:450–455

Shell L, Rozum M, Jortner BS, Ehrich M (1992) Neurotoxicity of acrylamide and 2, 5-hexanedione in rats evaluated using a functional observational battery and pathological examination. Neurotoxicol Teratol 14:273–283

Sickles DW, Sperry AO, Testino A, Friedman M (2007) Acrylamide effects on kinesin-related proteins of the mitotic/meiotic spindle. Toxicol Appl Pharmacol 222:111–121

Suzuki K, Pfaff LD (1973) Acrylamide neuropathy in rats. An electron microscopic study of degeneration and regeneration. Acta Neuropathol 24:197–213

Takahashi M, Shibutani M, Inoue K, Fujimoto H, Hirose M, Nishikawa A (2008) Pathological assessment of the nervous and male reproductive systems of rat offspring exposed

maternally to acrylamide during the gestation and lactation periods—a preliminary study. J Toxicol Sci 33:11–24

Takahashi M, Shibutani M, Nakahigashi J, Sakaguchi N, Inoue K, Morikawa T, Yoshida M, Nishikawa A (2009) Limited lactational transfer of acrylamide to rat offspring on maternal oral administration during the gestation and lactation periods. Arch Toxicol 83:785–793

Tates AD, Dietrich AJJ, de Vogel N, Neuteboom I, Bos A (1983) A micronucleus method for detection of meiotic micronuclei in male germ cell of mammals. Mutat Res 121:131–138

Tice RR, Agurell E, Anderson D, Burlinson B, Hartmann A, Kobayashi H, Miyamae Y, Rojas Y, Ryu JC, Sasaki YF (2000) Single cell gel/comet assay: guidelines for in vitro and in vivo genetic toxicology testing. Environ Mol Mutagen 35:206–221

WHO/IPCS (2006) Summary and conclusions of the sixty-fourth meeting of the Joint FAO/WHO Expert Committee on Food Additives (JECFA) Rome, 8-17 February 2005. summary_report_64_final.pdf.Available from: http://www.who.int/ipcs/food/jecfa/summaries/en/i

Yousef MI, El-Demerdash FM (2006) Acrylamide-induced oxidative stress and biochemical perturbations in rats. Toxicology 219: 133–141

Zhang X, Cao J, Jiang L, Geng C, Zhong L (2009) Protective effect of hydroxytyrosol against acrylamide-induced cytotoxicity and DNA damage in HepG2 cells. Mutat Res 664:64–68

HIPPOCAMPUS 21:127–132 (2011)

RAPID COMMUNICATION

Hippocampal Epigenetic Modification at the Brain-Derived Neurotrophic Factor Gene Induced by an Enriched Environment

Naoko Kuzumaki,[1] Daigo Ikegami,[1] Rie Tamura,[1] Nana Hareyama,[1] Satoshi Imai,[1] Michiko Narita,[1] Kazuhiro Torigoe,[1] Keiichi Niikura,[1] Hideyuki Takeshima,[2] Takayuki Ando,[2] Katsuhide Igarashi,[3] Jun Kanno,[3] Toshikazu Ushijima,[2] Tsutomu Suzuki,[1*] and Minoru Narita[1*]

ABSTRACT: Environmental enrichment is an experimental paradigm that increases brain-derived neurotrophic factor (BDNF) gene expression accompanied by neurogenesis in the hippocampus of rodents. In the present study, we investigated whether an enriched environment could cause epigenetic modification at the BDNF gene in the hippocampus of mice. Exposure to an enriched environment for 3–4 weeks caused a dramatic increase in the mRNA expression of BDNF, but not platelet-derived growth factor A (PDGF-A), PDGF-B, vascular endothelial growth factor (VEGF), nerve growth factor (NGF), epidermal growth factor (EGF), or glial fibrillary acidic protein (GFAP), in the hippocampus of mice. Under these conditions, exposure to an enriched environment induced a significant increase in histone H3 lysine 4 (H3K4) trimethylation at the BDNF P3 and P6 promoters, in contrast to significant decreases in histone H3 lysine 9 (H3K9) trimethylation at the BDNF P4 promoter and histone H3 lysine 27 (H3K27) trimethylation at the BDNF P3 and P4 promoters without any changes in the expression of their associated histone methylases and demethylases in the hippocampus. The expression levels of several microRNAs in the hippocampus were not changed by an enriched environment. These results suggest that an enriched environment increases BDNF mRNA expression via sustained epigenetic modification in the mouse hippocampus. © 2010 Wiley-Liss, Inc.

KEY WORDS: mouse hippocampus; epigenome; BDNF gene; neurogenesis; environmental enrichment

INTRODUCTION

Over the past few decades, exposure to an enriched environment, which consists of housing groups of animals together in a complex environment with various toys to provide more opportunity for learning and social interaction than standard laboratory living conditions, has been shown to enhance behavioral performance in various learning tasks. Consistent with these behavioral tests, exposure to an enriched environment has been shown to induce biochemical and structural changes in the hippocampal dentate gyrus (DG) and CA1 region, such as an increased number of dendritic branches and spines, enlargement of synapses, and an increased number of glial cells. Moreover, exposure of adult rodents to increased environmental complexity induces hippocampal progenitor proliferation and neurogenesis (Nilsson et al., 1999; van Praag et al., 1999). However, the detailed mechanisms that control neurogenesis in the hippocampus of animals housed in an enriched environment are still unclear.

It has been reported that brain-derived neurotrophic factor (BDNF) promotes neuronal differentiation from endogenous progenitor cells in the ventricular wall of the adult forebrain (Ahmed et al., 1995; Kirschenbaum and Goldman, 1995), and the increased expression of BDNF is required for the environmental induction of hippocampal neurogenesis in rodents (Rossi et al., 2006). The BDNF gene and the regulation of its expression are highly complex, and have been examined in both human and rodent brains (Timmusk et al., 1993; Liu et al., 2006; Aid et al., 2007; Pruunsild et al., 2007). The mouse BDNF gene, which shows a high degree of sequence homology to its human congener, contains multiple 5′ noncoding exons and a single 3′ coding exon for the mature BDNF protein (Aid et al., 2007). These noncoding exons undergo alternative splicing with the common coding exon to produce multiple exon-specific BDNF transcripts. Nine BDNF promoters have been previously identified in the mouse (Aid et al., 2007), and each drives the transcription of BDNF mRNAs containing one of the four 5′ noncoding exons (I, II, III, IV, V, VI, VII, or VIII) spliced to the common 3′ coding exon.

[1] Department of Toxicology, Hoshi University School of Pharmacy and Pharmaceutical Sciences, 2-4-41 Ebara, Shinagawa-ku, Tokyo 142-8501, Japan; [2] Carcinogenesis Division, National Cancer Center Research Institute, 5-1-1 Tsukiji, Chuo-ku, Tokyo 104-0045, Japan; [3] Division of Cellular and Molecular Toxicology, Biological Safety Research Center, National Institute of Health Sciences, 1-18-1, Kamiyoga, Setagaya-ku, Tokyo 154-0000, Japan
Additional Supporting Information may be found in the online version of this article.
Grant sponsor: Ministry of Education, Culture, Sports, Science and Technology of Japan
*Correspondence to: Minoru Narita, Ph.D., Department of Toxicology, Hoshi University School of Pharmacy and Pharmaceutical Sciences, 2-4-41 Ebara, Shinagawa-ku, Tokyo 142-8501, Japan. E-mail: narita@hoshi.ac.jp and Tsutomu Suzuki, Ph.D., Department of Toxicology, Hoshi University School of Pharmacy and Pharmaceutical Sciences, 2-4-41 Ebara, Shinagawa-ku, Tokyo 142-8501, Japan. E-mail: suzuki@hoshi.ac.jp
Accepted for publication 22 December 2009
DOI 10.1002/hipo.20775
Published online 15 March 2010 in Wiley Online Library (wileyonlinelibrary.com).

Chromatin remodeling at gene promoter regions is becoming increasingly recognized as a key control point of gene expression. Histone modification represents one prominent form of chromatin remodeling. According to the "histone code theory," different modifications of histones at a particular promoter region, alone or in combination, define a specific epigenetic state that encodes gene activation vs. gene silencing (Jenuwein and Allis, 2001). Intriguing correlations have been found between cellular plasticity, including transformation and such epigenetic modification at a specific gene (Kouzarides, 2007; Borrelli et al., 2008), indicating that possible epigenetic modification at BDNF gene promoters may partly contribute to adult neurogenesis. Therefore, in the present study, we evaluated whether an enriched environment could induce histone modification at several BDNF gene promoters in mice.

Male C57BL/6J mice (Jackson Laboratory), weighing 18–23 g, were used in the present study. Control mice were housed four per standard (16.5 × 26.5 × 13.5 cm^3) plexiglass cage. Mice

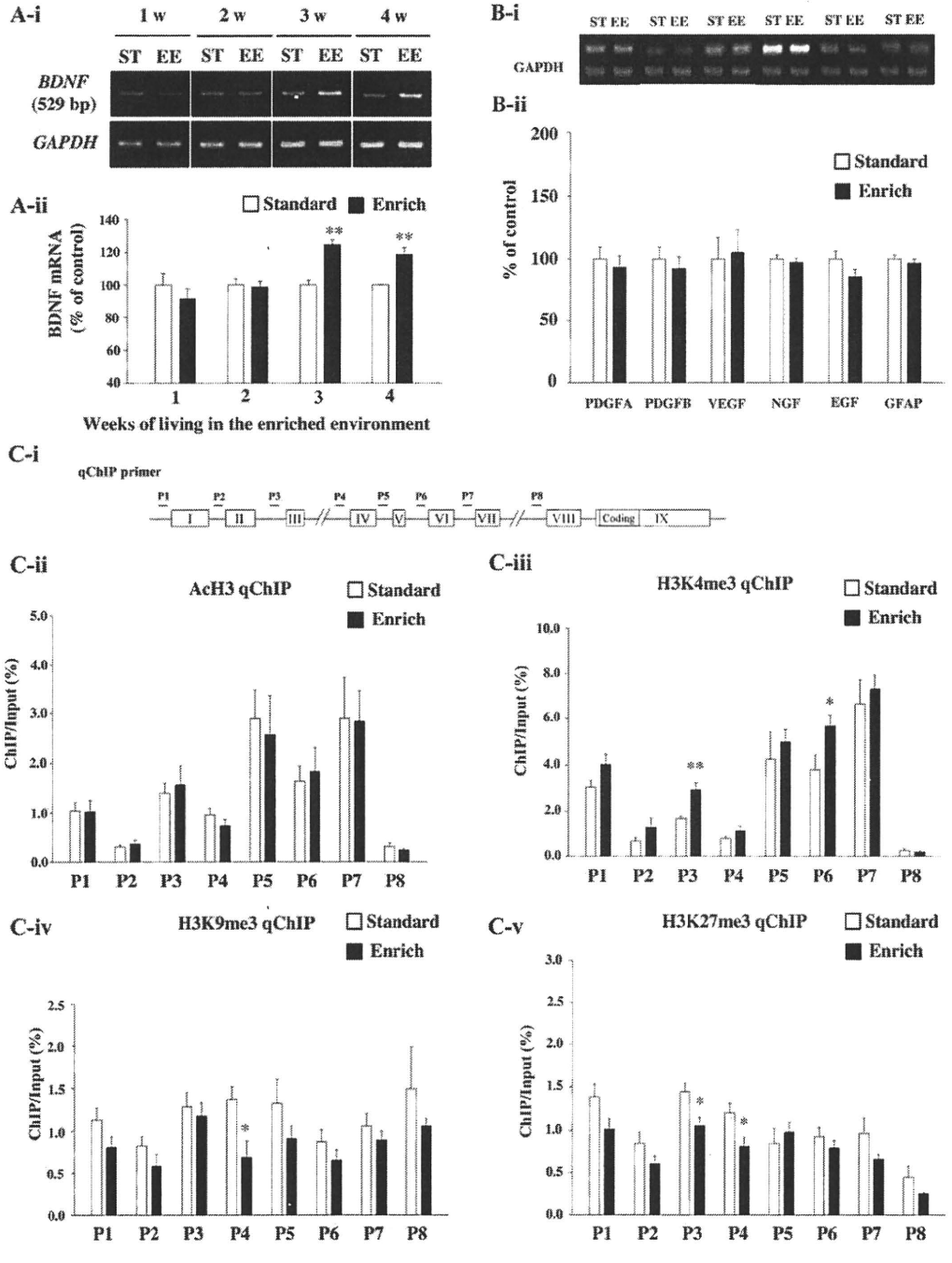

in the enriched environment group were kept eight per large (25.5 × 42.5 × 39 cm^3) wire-mesh, two-storied cage, which contained tunnels and running wheels, for 4 weeks (Supporting Information Fig. 1A).

In the DG of mice housed in the enriched environment for 4 weeks, immunoreactivity (IR) for doublecortin, which is a microtubule-associated protein that is expressed specifically in virtually all migrating neuronal precursors of the CNS and which has been used as a candidate marker for neural migration and differentiation, was increased compared to that in mice housed in the standard cage (Supporting Information Fig. 1B). Furthermore, IR for NeuroD, which is another marker for the differentiation of granule cells in the hippocampus (Miyata et al., 1999), was clearly increased in the DG of mice housed in an enriched environment (Supporting Information Fig. 1C). Additionally, the number of BrdU-positive cells in the DG that were classified as newly dividing cells was markedly increased in mice housed in an enriched environment (Supporting Information Fig. 2A), and theses were clearly colocalized with the neuronal marker NeuN (Supporting Information Fig. 2B). In paralleled with adult neurogenesis, the expression of BDNF mRNA in the hippocampus was significantly elevated after exposure to an enriched environment for both 3 and 4 weeks (Fig. 1A). In contrast, mRNA levels of glial fibrillary acidic protein (GFAP), platelet-derived growth factor A (PDGF-A), PDGF-B, vascular endothelial growth factor (VEGF), nerve growth factor (NGF), and epidermal growth factor (EGF) in the hippocampus were not altered by exposure to an enriched environment for 4 weeks (Fig. 1B).

Under these conditions, a significant increase in histone H3 lysine 4 (H3K4) trimethylation at the BDNF P3 and P6 promoters was observed upon exposure to an enriched environment for 4 weeks. Furthermore, significant decreases in histone H3 lysine 9 (H3K9) trimethylation at the BDNF P4 promoter, and histone H3 lysine 27 (H3K27) trimethylation at the BDNF P3 and P4 promoters were seen in the hippocampus of mice under an enriched environment. In contrast, an enriched environment did not produce the hyperacetylation of H3 in the hippocampus of enriched mice (Fig. 1C).

In terms of changes in mRNA levels of several histone methylases and demethylases in the hippocampus, an enriched environment failed to change the mRNA expression of MLL1, LSD1, Jarid1a, Jarid1b, jmjd2B, jmjd2C, jmjd2D, EZH2, UTX, or jmjd3 (Fig. 2A).

As with histone methylases and demethylases, no significant changes in microRNA9 (miR9), miR124a, miR132, miR133b, or miR145 were observed in the hippocampus of mice housed in an enriched environment for 2 and 4 weeks compared to mice housed in a standard cage (Fig. 2B).

In the present study, we demonstrated hippocampal neurogenesis in mice that were exposed to an enriched environment. This notion is supported by previous reports that exposure of adult rodents to an enriched environment increased neurogenesis in the hippocampus (Kempermann et al., 1997; Nilsson et al., 1999).

During development, growth factors provide important extracellular signals that regulate the proliferation and differentiation of neural stem cells in the CNS (Calof, 1995). Several investigations have examined the role of these factors in the adult brain (Calof, 1995; Kuhn et al., 1997). Furthermore, it has been shown that exposure to an enriched environment increased the expression of BDNF genes (Falkenberg et al., 1992). In support of these findings, the present study showed that the expression of BDNF mRNA in the hippocampus was significantly elevated after exposure to an enriched environment for both 3 and 4 weeks. In contrast, mRNA levels of GFAP, PDGF-A, PDGF-B, VEGF, NGF, and EGF in the hippocampus were not altered under the present conditions. In our *in vitro* study using neural stem cells cultured from the mouse embryonic forebrain, neuronal differentiation was clearly observed following exposure to recombinant BDNF (Supporting Information Fig. 3). These findings raise the possibility that an enriched environment may stimulate expression of the BDNF gene in the hippocampus and, in turn, the enhanced

FIGURE 1. (A) Time course of changes in the expression of BDNF mRNA in the hippocampus. (A-i) Representative RT-PCR for BDNF mRNA in the hippocampus obtained from standard or enriched mice. (A-ii) The intensity of the bands was semiquantified using NIH Image software. The value for BDNF mRNA was normalized by that for the internal standard glyceraldehyde-3-phosphate dehydrogenase (GAPDH) mRNA. The value for enriched mice is expressed as a percentage of the increase in standard mice. Each column represents the mean ± S.E.M. of six samples. **$P < 0.01$ vs. the standard group. (B) Upper: Representative RT-PCR for PDGFA, PDGFB, VEGF, NGF, EGF, and GFAP mRNAs in the hippocampus obtained from standard or enriched mice. Lower: The values for mRNAs were normalized by that for GAPDH mRNA. Each column represents the mean ± S.E.M. of six samples. (C-i) Schematic of the BDNF gene: The BDNF gene contains eight noncoding exons I–VIII upstream of the coding exon IX in mouse. Exons I–VIII can each be alternatively spliced next to exon IX, from the 5′ UTR region of different mRNA splice variants, BDNF I-VIII, which can promote the expression of their corresponding transcript variants. For an mRNA analysis of total BDNF, primers were used to amplify exon IX. For ChIP analysis, primers were designed around the putative promoters, P1-P8, which are located upstream of exons I–VIII. (C-ii, iii, iv, v) Stable changes in histone modifications in the hippocampus in mice housed under standard or enriched conditions for 4 weeks. ChIP assays were performed to measure the levels of several histone modifications at the eight BDNF promoters Ex1-Ex8 (P1–8) in the hippocampus using specific antibodies for each modification state. Levels of promoter enrichment were quantified by quantitative PCR. (C-ii) Histone H3 was not altered at BDNF P1–P8. (C-iii) Histone H3K4 trimethylation was increased at BDNF P3 and P6 in mice housed under enriched conditions for 4 weeks. *$P < 0.05$ vs. the standard group, **$P < 0.01$ vs. the standard group. (C-iv) H3K9 trimethylation was decreased at BDNF P4 in mice housed under enriched conditions for 4 weeks. *$P < 0.05$ vs. the standard group. (C-v) Histone H3K27 trimethylation was decreased at BDNF P3 and P4 in mice housed under enriched conditions for 4 weeks. *$P < 0.05$ vs. the standard group.

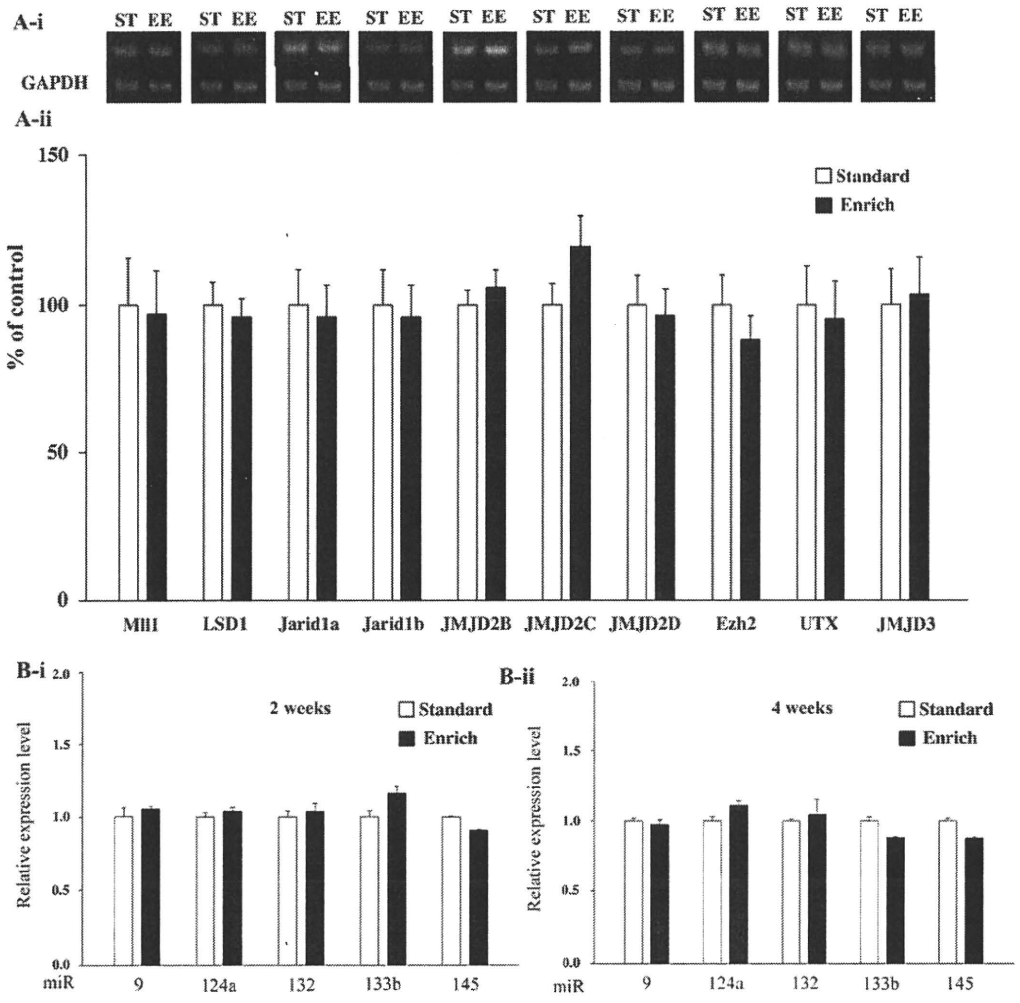

FIGURE 2. **(A) Upper: Representative RT-PCR for MLL1 (an H3K4 methyltransferase), LSD1, Jarid1a, and Jarid1b (H3K4 demethylases), JMJD2B, JMJD2C and JMJD2D (H3K9 demethylases), Ezh2 (H3K27 methyltransferase), and UTX and JMJD3 (H3K27 demethylases). mRNAs in the hippocampus obtained from standard or enriched mice. Lower: The value for mRNA was normalized by that for GAPDH mRNA. Each column represents the mean ± SEM of six samples. (B) Expression levels of miRNAs were measured in the hippocampus of mice housed in an enriched environment for 2 weeks (B-i) and 4 weeks (B-ii). The value for miRNA was normalized by that for the internal standard snoRNA202.**

BDNF protein may lead to neural differentiation from its precursors in the hippocampal DG.

We next evaluated whether an enriched environment increases BDNF gene expression through chromatin-specific events that promote the expression of distinct transcript variants. In this study we analyzed two active histone modifications (acetylation of histone H3, AcH3, and trimethylation of H3K4) and two repressive histone modifications (trimethylation of H3K9 and trimethylation of H3K27) at different BDNF promoter regions in the hippocampus. As a result, we detected a significant increase in H3K4 trimethylation, an activated histone modification marker, at the BDNF P3 and P6 promoters after exposure to an enriched environment for 4 weeks. Furthermore, significant decreases in H3K9 trimethylation, a repressive histone modification marker, at the BDNF P4 promoter, and H3K27 trimethylation, another repressive histone modification marker, at the BDNF P3 and P4 promoters were seen after exposure to an enriched environment. Under these conditions, we observed that an enriched environment did not produce the hyperacetylation of H3 in enriched mice.

The methylation of H3K9 and H3K27 can be directly modulated by histone methylases and demethylases that target specific lysine residues and methylation states (Jenuwein and Allis, 2001; Kouzarides, 2007). Thus, we investigated whether an enriched environment could alter the mRNA level of several histone methylases and demethylases in the hippocampus. We found that an enriched environment did not change the

mRNA expression of MLL1 (an H3K4 methyltransferase), LSD1, Jarid1a or Jarid1b (H3K4 demethylases), jmjd2B, jmjd2C or jmjd2D (H3K9 demethylases), EZH2 (an H3K27 methyltransferase), or UTX or jmjd3 (H3K27 demethylases).

Recently, microRNAs (miRNAs), a class of small, noncoding RNAs, have been identified as important regulators of many biological processes, including organogenesis and disease development (Kim et al., 2007; Chen et al., 2008; Hutchison et al., 2009). Indeed, it has been shown that epigenetic factors such as DNA methylation, histone modification, and regulatory noncoding RNAs affect the fate of neural stem cells (Chi and Bernstein, 2009). miRNAs have the potential to specifically regulate a large set of target molecules, which may affect the cell's fate in a programmatic way, and the role of miRNAs in stem cell gene networks is being actively explored. Their ability to potentially regulate large numbers of target genes simultaneously suggests that they may be important sculptors of transcriptional networks. In this study, we found that miR9, miR124a, miR132, miR133b, and miR145 are expressed in the hippocampus of adult mice. It has been reported that miR145 regulates Oct4, Sox2, and Klf4 and suppresses the potential of human embryonic stem cells to generate any differentiated cell type (pluripotency) (Xu et al., 2009). miR124, one of these signature miRNAs that is enriched in the brain, regulates adult neurogenesis in the subventricular zone stem cell niche (Cheng et al., 2009). miR132 is localized and synthesized, in part, at synaptic sites in dendrites to regulate synaptic formation and plasticity (Vo et al., 2005). miR9 is expressed specifically in the hippocampus and may be involved in neural stem cell self-renewal and differentiation (Krichevsky et al., 2006; Bak et al., 2008). In the present study, there were no significant changes in miR9, miR124a, miR132, miR133b, or miR145 in the hippocampus of mice housed in an enriched environment for 2 and 4 weeks compared to mice housed in a standard cage. Although further studies are required to investigate the molecular mechanism of hippocampal neurogenesis induced by an enriched environment, we propose that an enriched environment may increase BDNF expression accompanied by histone modification without directly changing the expression of histone H3 methylases and demethylases, and miRs in the hippocampus.

In conclusion, the present study demonstrated that an enriched environment stimulates neuronal differentiation from precursors in the hippocampal DG. Furthermore, the increased expression of BDNF was observed in the hippocampus of mice that had been exposed to an enriched environment. This enrichment induced a significant increase in H3K4 trimethylation at the BDNF P3 and P6 promoters and a significant decrease in H3K9 trimethylation at the BDNF P4 promoter and H3K27 trimethylation at the BDNF P3 and P4 promoters in the hippocampus of mice. These results suggest that an enriched environment may increase BDNF expression with notably sustained chromatin regulation in the mouse hippocampus. This phenomenon could partly explain the hippocampal neurogenesis induced by an enriched environment in mice.

Acknowledgment

The authors thank Dr. Kazuya Miyagawa for their expert technical assistance.

REFERENCES

Ahmed S, Reynolds BA, Weiss S. 1995. BDNF enhances the differentiation but not the survival of CNS stem cell-derived neuronal precursors. J Neurosci 15:5765–5778.

Aid T, Kazantseva A, Piirsoo M, Palm K, Timmusk T. 2007. Mouse and rat BDNF gene structure and expression revisited. J Neurosci Res 85:525–535.

Bak M, Silahtaroglu A, Moller M, Christensen M, Rath MF, Skryabin B, Tommerup N, Kauppinen S. 2008. MicroRNA expression in the adult mouse central nervous system. RNA 14:432–444.

Borrelli E, Nestler EJ, Allis CD, Sassone-Corsi P. 2008. Decoding the epigenetic language of neuronal plasticity. Neuron 60:961–974.

Calof AL. 1995. Intrinsic and extrinsic factors regulating vertebrate neurogenesis. Curr Opin Neurobiol 5:19–27.

Chen X, Zhang J, Fang Y, Zhao C, Zhu Y. 2008. Ginsenoside Rg1 delays tert-butyl hydroperoxide-induced premature senescence in human WI-38 diploid fibroblast cells. J Gerontol A Biol Sci Med Sci 63:253–264.

Cheng LC, Pastrana E, Tavazoie M, Doetsch F. 2009. miR-124 regulates adult neurogenesis in the subventricular zone stem cell niche. Nat Neurosci 12:399–408.

Chi AS, Bernstein BE. 2009. Developmental biology. Pluripotent chromatin state. Science 323:220–221.

Falkenberg T, Mohammed AK, Henriksson B, Persson H, Winblad B, Lindefors N. 1992. Increased expression of brain-derived neurotrophic factor mRNA in rat hippocampus is associated with improved spatial memory and enriched environment. Neurosci Lett 138:153–156.

Hutchison ER, Okun E, Mattson MP. 2009. The therapeutic potential of microRNAs in nervous system damage, degeneration, and repair. Neuromolecular Med 11:153–161.

Jenuwein T, Allis CD. 2001. Translating the histone code. Science 293:1074–1080.

Kempermann G, Kuhn HG, Gage FH. 1997. More hippocampal neurons in adult mice living in an enriched environment. Nature 386:493–495.

Kim J, Inoue K, Ishii J, Vanti WB, Voronov SV, Murchison E, Hannon G, Abeliovich A. 2007. A MicroRNA feedback circuit in midbrain dopamine neurons. Science 317:1220–1224.

Kirschenbaum B, Goldman SA. 1995. Brain-derived neurotrophic factor promotes the survival of neurons arising from the adult rat forebrain subependymal zone. Proc Natl Acad Sci USA 92:210–214.

Kouzarides T. 2007. Chromatin modifications and their function. Cell 128:693–705.

Krichevsky AM, Sonntag KC, Isacson O, Kosik KS. 2006. Specific microRNAs modulate embryonic stem cell-derived neurogenesis. Stem Cells 24:857–864.

Kuhn HG, Winkler J, Kempermann G, Thal LJ, Gage FH. 1997. Epidermal growth factor and fibroblast growth factor-2 have different effects on neural progenitors in the adult rat brain. J Neurosci 17:5820–5829.

Liu QR, Lu L, Zhu XG, Gong JP, Shaham Y, Uhl GR. 2006. Rodent BDNF genes, novel promoters, novel splice variants, and regulation by cocaine. Brain Res 1067:1–12.

Miyata T, Maeda T, Lee JE. 1999. NeuroD is required for differentiation of the granule cells in the cerebellum and hippocampus. Genes Dev 13:1647–1652.

Nilsson M, Perfilieva E, Johansson U, Orwar O, Eriksson PS. 1999. Enriched environment increases neurogenesis in the adult rat dentate gyrus and improves spatial memory. J Neurobiol 39:569–578.

Pruunsild P, Kazantseva A, Aid T, Palm K, Timmusk T. 2007. Dissecting the human BDNF locus: Bidirectional transcription, complex splicing, and multiple promoters. Genomics 90:397–406.

Rossi C, Angelucci A, Costantin L, Braschi C, Mazzantini M, Babbini F, Fabbri ME, Tessarollo L, Maffei L, Berardi N, Caleo M. 2006. Brain-derived neurotrophic factor (BDNF) is required for the enhancement of hippocampal neurogenesis following environmental enrichment. Eur J Neurosci 24:1850–1856.

Timmusk T, Palm K, Metsis M, Reintam T, Paalme V, Saarma M, Persson H. 1993. Multiple promoters direct tissue-specific expression of the rat BDNF gene. Neuron 10:475–489.

van Praag H, Kempermann G, Gage FH. 1999. Running increases cell proliferation and neurogenesis in the adult mouse dentate gyrus. Nat Neurosci 2:266–270.

Vo N, Klein ME, Varlamova O, Keller DM, Yamamoto T, Goodman RH, Impey S. 2005. A cAMP-response element binding protein-induced microRNA regulates neuronal morphogenesis. Proc Natl Acad Sci USA 102:16426–16431.

Xu N, Papagiannakopoulos T, Pan G, Thomson JA, Kosik KS. 2009. MicroRNA-145 regulates OCT4, SOX2, and KLF4 and represses pluripotency in human embryonic stem cells. Cell 137:647–658.

SYNAPSE 64:611–616 (2010)

Hippocampal Epigenetic Modification at the Doublecortin Gene is Involved in the Impairment of Neurogenesis With Aging

NAOKO KUZUMAKI,[1] DAIGO IKEGAMI,[1] RIE TAMURA,[1] TAKUYA SASAKI,[1] KEIICHI NIIKURA,[1] MICHIKO NARITA,[1] KAZUHIKO MIYASHITA,[1] SATOSHI IMAI,[1] HIDEYUKI TAKESHIMA,[2] TAKAYUKI ANDO,[2] KATSUHIDE IGARASHI,[3] JUN KANNO,[3] TOSHIKAZU USHIJIMA,[2] TSUTOMU SUZUKI,[1]* AND MINORU NARITA[1]*

[1]*Department of Toxicology, Hoshi University School of Pharmacy and Pharmaceutical Sciences, Shinagawa-Ku, Tokyo 142-8501, Japan*

[2]*Carcinogenesis Division, National Cancer Center Research Institute, Chuo-Ku, Tokyo 104-0045, Japan*

[3]*Division of Cellular and Molecular Toxicology, Biological Safety Research Center, National Institute of Health Sciences, Setagaya-Ku, Tokyo 154-0000, Japan*

KEY WORDS senescent; mouse hippocampus; epigenome; DCX; neurogenesis

ABSTRACT Recent research has suggested that epigenetic mechanisms, which exert lasting control over gene expression without altering the genetic code, could mediate stable changes in brain function. A growing body of evidence supports the idea that epigenetic changes play a role in the etiology of aging and its associated brain dysfunction. The present study was undertaken to evaluate the age-related changes in the expression of doublecortin, which is a marker for neuronal precursors, along with epigenetic modification in the hippocampus of aged mice. In the present study, the doublecortin-positive cells were almost completely absent from the dentate gyrus of the hippocampus of 28-month-old mice. Furthermore, the expression level of doublecortin mRNA was significantly decreased in the hippocampus of aged mice. Under these conditions, a significant decrease in H3K4 trimethylation and a significant increase in H3K27 trimethylation at doublecortin promoters were observed with aging without any changes in the expression of their associated histone methylases and demethylases in the hippocampus. These findings suggest that aging produces a dramatic decrease in the expression of doublecortin along with epigenetic modifications in the hippocampus. **Synapse 64:611–616, 2010.**

INTRODUCTION

Since the average human life span has increased dramatically over the last century, there are growing concerns about malfunctions associated with aging. The dysfunction of neurotransmission in normal aging and neuropsychiatric diseases late in life may contribute to the behavioral changes commonly observed in the elderly.

Neurogenesis occurs in specific areas in the adult brain throughout life, e.g., in the subventricular zone at the telencephalic level and in the dentate gyrus of the hippocampus (Eriksson et al., 1998; Lois and Alvarez-Buylla, 1993). The dentate gyrus, the hippocampus proper, and the subiculum constitute the hippocampal formation, which is critical for certain forms of learning and memory (Bliss and Collingridge, 1993). A positive correlation has been established between neurogenesis in the dentate gyrus and an animal's performance in behavioral tasks (Kempermann et al., 1997; van Praag et al., 1999). Aging is associated with a progressive accumulation of damaged molecules and impaired energy metabolism in brain cells. Neurons and glial cells may adapt to the adversities of aging by compensating for lost or damaged cells by producing new neurons and glia, and remodeling neuronal circuits.

The influence of age on rates of neurogenesis has been studied by several groups (Kuhn et al., 1996; Lichtenwalner et al., 2001). Changes in the relative proportion of young dentate gyrus neurons may have important consequences for hippocampal function and could possibly contribute to age-dependent structural

*Correspondence to: Minoru Narita, PhD, or Tsutomu Suzuki, PhD, Department of Toxicology, Hoshi University School of Pharmacy and Pharmaceutical Sciences, Tokyo. E-mail: narita@hoshi.ac.jp/suzuki@hoshi.ac.jp

Received 14 October 2009; Accepted 17 November 2009

DOI 10.1002/syn.20768

Published online 17 March 2010 in Wiley InterScience (www.interscience.wiley.com).

and functional hippocampal deficits (Barnes, 1994; Geinisman et al., 1992).

Epigenetic changes involve transmissible alterations in gene expression caused by mechanisms other than changes in the DNA sequence. (Gravina and Vijg, 2009) Epigenetic information is destined to change during development and in the course of essential somatic functions. This makes it a more likely candidate for errors than its more stable DNA-sequence counterpart, changes in which have been well documented and increase during aging (Gravina and Vijg, 2009). Indeed, epegenomic alterations are now becoming increasingly recognized as part of aging and its associated pathologic phenotypes (Gravina and Vijg, 2009). To better understand such age-dependent epigenetic modification, in this study we focused on the decreased expression of doublecortin, which is frequently used as a marker of a migrated neuronal progenitor in the hippocampus of aged mice.

This study was conducted in accordance with the Guiding Principles for the Care and Use of Laboratory Animals, Hoshi University, as adopted by the Committee on Animal Research of Hoshi University, which is accredited by the Ministry of Education, Culture, Sports, Science and Technology of Japan. All efforts were made to minimize the number of animals used and their suffering.

Two- and from 24- to 28-month-old C57BL/6J mice were used in the present study. Animals were kept in a room with an ambient temperature of 23 ± 1°C and a 12-h light/dark cycle (lights on 8:00 AM to 8:00 PM). Food and water were available ad libitum.

Mice were deeply anesthetized with isoflurane (3%) and perfusion-fixed with 4% paraformaldehyde (pH 7.4). The brain was then removed quickly and the hippocampus was rapidly dissected and postfixed in 4% paraformaldehyde for 2 h. The hippocampus was permeated with 20% sucrose for 1 day and 30% sucrose for 2 days, and then frozen in an embedding compound (Sakura Finetechnical, Tokyo, Japan). All samples were stored at −30°C until use. The sections were cut transversely at a thickness of 8 μm on a cryostat (Leica CM1510, Leica Microsystems, Heidelberg, Germany). The hippocampus sections were blocked in 5% normal goat serum in 0.01 M·phosphate-buffered saline (PBS) for 1 h at room temperature. Each primary antibody was diluted in 0.01 M PBS containing 5% normal goat serum (guinea pig polyclonal antibody to doublecortin [1:3500; Abcam Ltd., Cambridge, UK]), and incubated for two days overnight at 4°C. The samples were then rinsed and incubated with the appropriate secondary antibody conjugated with Alexa 488 for 2 h at room temperature. The slides were then coverslipped with PermaFluor Aqueous mounting medium (Immunon, Pittsburgh, PA). Fluorescence of immunolabeling was detected using a light microscope (Olympus AX-70; Olympus, Tokyo, Japan, and a Radiance 2000 laser-scanning microscope; BioRad, Richmond, CA), and photographed with a digital camera (Polaroid PDMCII/OL; Olympus).

Total RNA in the hippocampus of aged mice was extracted using the SV Total RNA Isolation system (Promega, Madison, WI) following the manufacturer's instructions. Purified total RNA was quantified spectrophotometrically at A_{260}. To prepare first-strand cDNA, 1 μg of RNA was incubated in 100 μl of buffer containing 10 mM dithiothreitol, 2.5 mM $MgCl_2$, dNTP mixture, 50 U of reverse transcriptase II (Invitrogen, Carlsbad, CA), and 0.1 mM oligo-$dT_{12\text{-}18}$ (Invitrogen). Each gene was amplified in 50 μl of PCR solution containing 0.8 mM $MgCl_2$, dNTP mixture, and DNA polymerase with synthesized primers (Table I). Samples were heated to 95°C for 1 min, 55°C for 2 min, and 72°C for 3 min. The final incubation was at 72°C for 7 min. The mixture was run on 2% agarose gel electrophoresis with the indicated markers and primers for the internal standard glyceraldehyde-3-phosphate dehydrogenase. The agarose gel was stained with ethidium bromide and photographed with UV transillumination. The intensity of the bands was analyzed and semiquantified by computer-assisted densitometry using ImageJ software. Values represent the mean ± SEM of three independent experiments.

TABLE I. Comprehensive List of All Primer Sequences Used

Experiment	Name	Sequence
RT-PCR	DCX	F: CTTTTGGTTCAGCAGAAGGG
		R: CAAATGTTCTGGGAGGCACT
	GFAP	F: ACAACTTTGCACAGGACCTC
		R: CGATTCAACCTTTCTCTCCA
	BDNF	F: TCACTGGCTGACACTTTTGAG
		R: CTATCCTTATGAATCGCCAGC
	MLL1	F: AGCGGAGAGGATGAGCAGT
		R: CGAGGTTTTCGAGGACTAGC
	LSD1	F: TCAACGTCCTCAATAATAAACCTGT
		R: CCTGAGTTTTCACTATCTTCTTCCA
	Jaridla	F: CCTCCATTTGCCTGTGAAGT
		R: CCTTTGCTGGCAACAATCTT
	Jaridlb	F: AGAGGCTGAATGAGCTGGAG
		R: TGGCAATTTTGGTCCATTTT
	jmjd2A	F: GACCACACTCTGCCCACAC
		R: TCCTGGGGTATTTCCAGACA
	jmjd2B	F: GGCTTTAACTGCGCTGAGTC
		R: GTGTGGTCCAGCACTGTGAG
	jmjd2C	F: CACGGAGGACATGGATCTCT
		R: CGAAGGGAATGCCATACTTC
	jmjd2D	F: GTCTTGGTCGTCGTCCTTGT
		R: AATCCCCCTTCAGAAGCTGT
	EZH2	F: GCCAGACTGGGAAGAAATCTG
		R: TGTGCTGGAAAATCCAAGTCA
	UTX	F: ATCCCAGCTCAGCAGAAGTT
		R: GGAGGAAAGAAAGCATCACG
	jmjd3	F: CCCCCATTTCAGCTGACTAA
		R: CTGGACCAAGGGGTGTGTT
	GAPDH	F: CCCCACGGCAAGTTCAACGG
		R: CTTTCCAGAGGGCCATCCA
Real-time PCR	DCX	F: CTTTTGGTTCAGCAGAAGGG
		R: CAAATGTTCTGGGAGGCACT
	β-actin	F: CAGCTTCTTTGCAGCTCCTT
		R: TCACCCACATAGGAGTCCTT
ChIP	DCX	F: AGCTTGCCTGTGCAATCTTT
		R: GAACACCCCCAACCTCCTAT

Fast SYBR Green Master Mix (2x) (Applied Biosystems, Inc., CA) was used as the basis for the reaction mixture in the real-time PCR assay. Each gene prepared by the above procedure was amplified in 20 μl of a PCR solution containing 10 μl of the Fast SYBR Green Master Mix (2x) with synthesized primers (Table I). In addition to each sample, each test run included a no-target control that contained reaction mixture and PCR-grade water. PCR with a StepOnePlus™ (Applied Biosystems, Inc., CA) was performed with the following cycling conditions: 95°C for 20 s, followed by 45 cycles of 95°C for 3 s and 60°C for 30 s. Fluorescence detection was conducted after each extension step.

A ChIP assay was performed as described previously (Takeshima et al., 2009; Tsankova et al., 2004) with minor modifications. Briefly, mouse hippocampus tissue was dissected as described above and cross-linked, and then tissue was lysed. Fifteen μg of soluble chromatin was incubated with 2 μg of specific antibodies against acetylated histone H3 (Millipore), H3K4 trimethylation (Wako Pure Chemicals, Osaka, Japan), H3K9 trimethylation (Millipore), H3K27 trimethylation (Millipore), overnight at 4°C. The immunocomplex was collected by Dynabeads Protein A (Invitrogen Dynal AS, Oslo, Norway), and DNA was recovered with RNaseA treatment; Proteinase K treatment followed by isopropanol precipitation. Immunoprecipitated DNA was dissolved in 50 μl of 1 × TE and 1 μl was used for quantitative PCR. Quantitative PCR was performed as described previously (Nakajima et al., 2009). The primers used are listed in Table I.

The data are expressed as the mean ± S.E.M. The statistical significance of differences between groups was assessed with Student's *t*-test (comparison of two groups) or an analysis of variance (ANOVA) followed by the Bonferroni test (comparison among multiple groups). A level of probability of 0.05 or less was considered significant.

Doublecortin is a cytoskeletal protein that is transiently expressed only in newborn neurons, and is used as a marker of neural progenitors. In agreement with a previous report (Hwang et al., 2008), we confirmed that doublecortin-positive cells were almost completely absent from the dentate gyrus of the hippocampus of 28-month-old mice (Fig. 1A). The level of doublecortin, the doublecortin mRNA was significantly decreased in the hippocampus of aged mice compared to that in young mice (Figs. 1B and 1C, $P < 0.001$ vs. young mice). In contrast, mRNA levels of glial fibrillary acidic protein (GFAP), a glial marker, and brain-derived .neurotrophic factor (BDNF) in the hippocampus were not altered by normal aging.

We next evaluated whether changes in doublecortin mRNA expression accompanied by aging could be regulated through chromatin-specific events. In this study, we analyzed two active histone modifications (acetylation of histone H3, AcH3, and trimethylation of lysine 4 on histone H3, H3K4) and two repressive histone modifications (trimethylation of lysine 9 on histone H3, H3K9, and trimethylation of lysine 27 on histone H3, H3K27) at doublecortin promoter regions in the hippocampus. As a result, we detected a significant decrease in H3K4 trimethylation at the doublecortin promoters with aging (Fig. 2A, $P < 0.05$ vs. young mice). Furthermore, a significant increase in H3K27 trimethylation at the doublecortin gene was seen with aging (Fig. 2A, $P < 0.05$ vs. young mice). Under these conditions, aging did not produce H3K9 trimethylation or hyperacetylation of H3 at the doublecortin gene (Fig. 2A).

The methylation of H3K9 and H3K27 can be directly modulated by histone methylases and demethylases that target specific lysine residues and methylation states. Thus, we finally investigated whether aging could alter the mRNA level of several histone methylases and demethylases in the hippocampus. We found that aging did not change the mRNA expression of MLL1 (a H3K4 methyltransferase), LSD1, Jarid1a or Jarid1b (H3K4 demethylases), jmjd2A, jmjd2B, jmjd2C or jmjd2D (H3K9 demethylases), EZH2 (a H3K27 methyltransferase), or UTX or jmjd3 (H3K27 demethylases) (Fig. 2B).

Doublecortin is a microtubule-associated protein that is expressed specifically in virtually all migrating neural precursors of the CNS and has been used as a candidate marker for neuronal migration and differentiation. In this study, aging caused a dramatic decrease in levels of doublecortin mRNA in the hippocampus. In the dentate gyrus of the hippocampus, few or no doublecortin-positive cells were observed by aging. These findings strongly suggest that an aging can stimulate the impairment of neuronal differentiation from precursors in the hippocampal dentate gyrus. These notions are supported by previous reports that aging promoted the impairment of neurogenesis (Kuhn et al., 1996; Lichtenwalner et al., 2001).

Epigenetic alterations of DNA play key roles in determining gene structure and expression (Jaenisch and Bird, 2003; Tsankova et al., 2007). A major epigenetic modification, chromatin remodeling, modulates gene expression with high temporal and spatial resolution by permitting small groups of nucleosomes to become more or less open, which consequently enhances or inhibits access of the transcriptional machinery to specific promoter regions. The acetylation and methylation of histone proteins at specific residues play a major role in chromatin remodeling. Lysine acetylation almost always correlates with chromatin accessibility and transcriptional activity, whereas lysine methylation can have different effects depending on which residue is modified. Trimethylation of H3K4

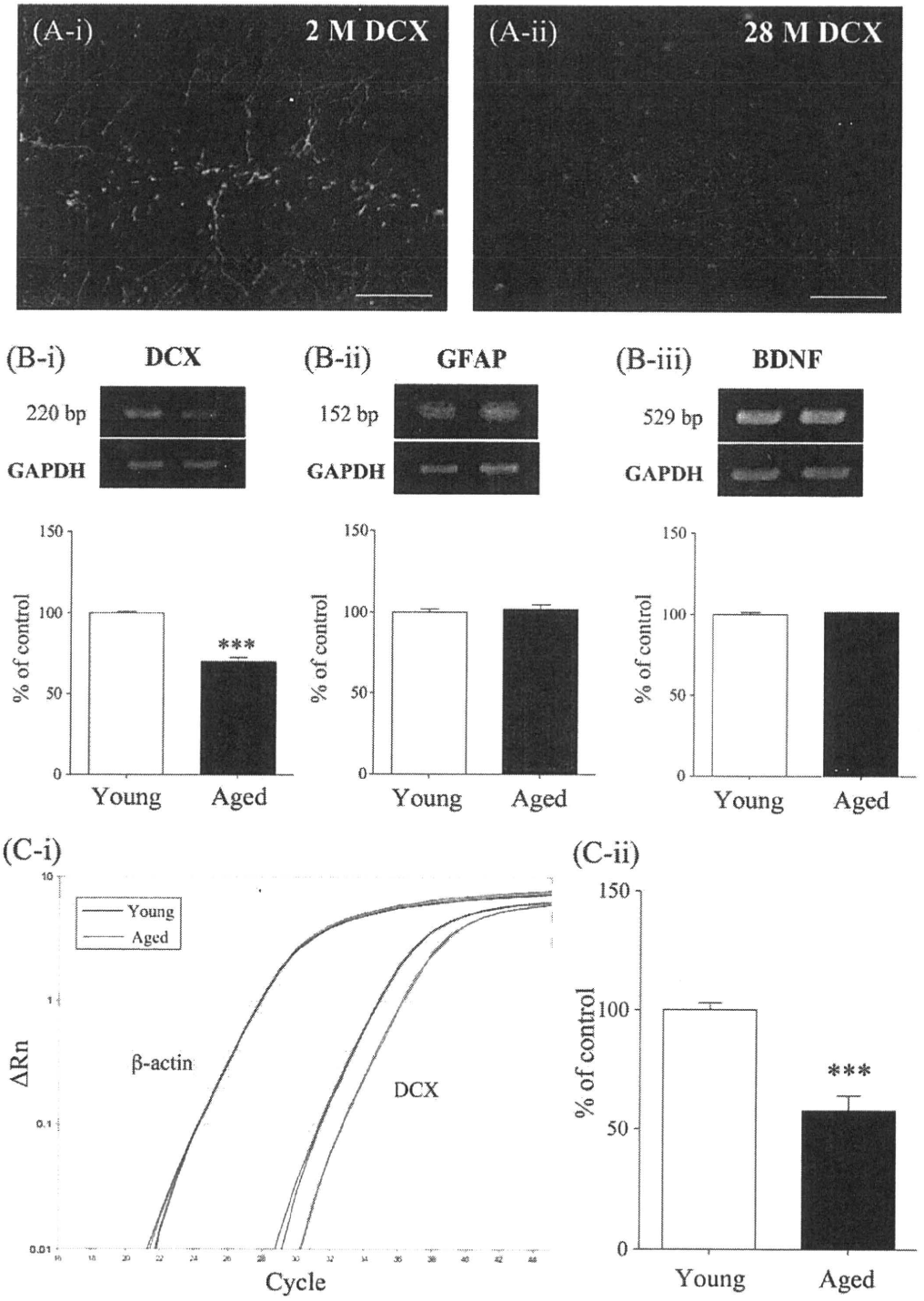

Fig. 1. (**A**) Immunofluorescent staining for doublecortin in the dentate gyrus in young and aged mice. Doublecortin-like immunoreactivity in the dentate gyrus of 28-month-old mice (A-ii) was decreased compared to that in 2-month-old mice (A-i). Scale bar: 50 μm. (**B**) Upper: Representative RT-PCR for doublecortin (DCX; B-i), GFAP (B-ii) and BDNF (B-iii) mRNAs in the hippocampus obtained from young and aged mice. Lower: The intensity of the bands was semiquantified using NIH Image software. The values for DCX, GFAP and BDNF mRNA were normalized by that for the internal standard glyceraldehyde-3-phosphate dehydrogenase (GAPDH) mRNA. The value for aged mice is expressed as a percentage of the increase in young mice. Each column represents the mean ± S.E.M. six samples. ***$P < 0.001$ vs. the young group. (**C**) Quantitative analysis of DCX mRNA in the hippocampus obtained from young and aged mice. (C-i) Amplification plots of fluorescence intensities vs. PCR cycle numbers in each sample. (C-ii) Each column represents the mean ± S.E.M. of three samples. ***$P < 0.001$ vs. the young group.